Accuracy evaluation of ionospheric delay from multi-scale reference networks and its application for fast PPP ambiguity resolution

Lewen Zhao[1,2], Douša Jan[1], Václavovic Pavel[1]

[1]Research Institute of Geodesy, Topography and Cartography, Zdiby, 25066, Czech Republic

[2]School of Remote Sensing and Geomatics Engineering, Nanjing University of Information Science and Technology, Nanjing, 210044, China

Correspondence to: Lewen Zhao[1,2] (lewen.zhao@pecny.cz)

https://doi.org/10.31490/9788024845050-14

Abstract

The Precise Point Positioning（PPP) can achieve a fast ambiguity resolution (PPP-RTK) when augmented with precise ionospheric delays derived from regional GNSS networks. In this study, the accuracy of the ionospheric delay derived from multi-scale networks are assessed and used for the GPS and Galileo PPP-RTK demonstration. First, the convergence time of the GPS-only PPP are evaluated based on the GFZ final and CNES real-time products. Results indicated that an average convergence time of 30 min and 20 min is needed for the CNES and GFZ float solutions, respectively, in order to achieve a decimetre level horizontal position accuracy. After applying the ambiguity resolution method, 20% and 35% improvements are observed reaching 24min and 13min, respectively. Then, the accuracy of ionospheric delays derived from the ambiguity-fixed PPP and the CODE global products are assessed. A short-baseline comparison indicated that the mean bias and standard deviation of the derived multi-day ionospheric errors are within 0.15 TECU and 0.06 TECU, respectively, with a presence of a daily periodic term. The accuracy of the interpolated ionospheric delay from global models are more related to the location of the stations, ranging from 1 TECU to 3 TECU. Finally, precise ionospheric delays derived from the EUREF permanent network with the inter-station distance larger than 73 km are selected for ionospheric modelling at the user location. Results indicated that the PPP ambiguity resolution can be achieved within a minute. After enlarging the inter-station distance to 209 km, ambiguity resolution can be achieved within several epochs with improved fixing rate as well.

Keywords: PPP-RTK, GNSS, fast-ambiguity resolution, ionospheric delay, G-Nut software

Introduction

Based on the real-time orbits and clock corrections estimated from global reference GNSS networks, precise point positioning (PPP) (Zumberge et al., 1997) can achieve decimetres to centimetres accuracy in kinematic model. However, a long convergence time of about 30 minutes (Geng et al., 2010) is needed which limits its widespread application, such as modern agriculture, mobile mapping and drone navigation. Precise point positioning ambiguity resolution (PPP-AR) with satellite phase biases correction (Ge et al., 2008) can shorten the convergence time and improve the accuracy significantly. However, a convergence time of about 15 minutes is still needed. One potential solution is to augment

PPP with precise ionospheric and tropospheric corrections using local network to achieve fast and reliable ambiguity resolution, which is the concept of PPP-RTK (G. Wubbena et al., 2005).

Precise atmosphere modelling is one key issue to enable the fast ambiguity resolution in PPP-RTK. De et al. (2017) assessed the performance of troposphere modelling with dense and sparse networks for GPS only and GPS+GLONASS ambiguity float PPP. Results indicated that convergence time can be shorten from 2% to 20% when considering different coordinate components and GNSS combinations. Psychas et al. (2018) assessed the precision of ionospheric corrections on fast ambiguity resolution. Results indicated that that faster PPP-RTK solutions can be achieved in case the precision of ionospheric corrections is better than 5 cm (~0.31 TECU) at a user side. The ionospheric delay derived from ambiguity-fixed PPP are used for regional ionospheric modelling with an inter-station distance of 50KM and can achieve an internal RMS of 1.1 TECU.

After obtaining the precise atmospheric corrections, these are interpolated and predicted to the user location, and the performance of PPP-RTK with different network scales has been assessed. Teunissen et al. (2010) demonstrated the performance of PPP-RTK based on a small scale network with inter-station distances of around 27 and 60 km and indicated that centimetre level positioning accuracy can be achieved which is comparable to network RTK solutions. Li et al. (2018) used linearly interpolated method for atmospheric corrections prediction and showed that instantaneous ambiguity resolution can be achieved at the user level from a regional network of 60 km distance. Zhang et al. (2011) further demonstrated the PPP-RTK performance with inter-station distances ranging from 60 to 100km. Li et al. (2020) demonstrated that the performance of PPP-RTK based on BDS/GPS observations using data in Europe during a calm ionospheric disturbance period. Results indicate that centimetre-level positioning accuracy can be achieved based on GPS- or BDS-only observations, and performance can be further improved by realizing PPP AR method. Psychas et al. (2020) analysed the real-time PPP-RTK user performance using ionospheric corrections from multi-scale regional networks during a day with medium ionospheric disturbance. Results showed that sub-10 cm horizontal accuracy can be achieved within 1 min and 2 min based on corrections from a network with 68 km and 115 km spacing.

PPP-RTK technology preserves the benefits of PPP for global positioning and RTK for a fast convergence. Besides, only one-way communication is needed which bring a great potential for its application using low-cost smart terminals. In this study, a raw PPP model is used to derive the clean ionospheric delay which is not affected by receiver and satellite hardware delays. The accuracy of the ionospheric delay derived from ambiguity-fixed PPP, as well the CODE global ionospheric products, are assessed. Then, the performance of GPS and Galileo-only PPP-RTK are assessed by comparing to the traditional ambiguity-float and ambiguity-fixed PPP solutions based on the data from EUREF network (Bruyninx et al., 2019). Finally, the conclusions are derived.

Data and models

Apart from the precise satellite orbits and clocks, satellite corrections of phase biases are necessary for the Precise Point Positioning (PPP) ambiguity resolution (PPP-AR). Since

2013, the international GNSS service (IGS) started providing an open-access real-time service (RTS), the National Centre for Space Studies (CNES) has been providing real-time orbits, clocks and phase biases for multi-GNSS (Laurichesse et al., 2016). Hence, this solution is first used for demonstrating of the performance of real-time PPP ambiguity resolution. Besides, the final orbits and clocks products from GFZ (Deng et al., 2016) completed with the phase biases estimated by GOP for demonstrating the performance of the PPP AR in a simulated real-time processing mode. Note that the difference of the two solutions remains mainly in the accuracy of the satellite products, not in the user solution.

For estimating phase biases at GOP using the G-Nut software (Václavovic et al. 2013), data from the MGEX permanent stations were processed on a daily basis in a sampling interval of 30 seconds with a simulation of real-time mode. The forward filter was thus applied only with an initial period for phase biases to converge. Strategies used for the processing at both service and user sides are listed in Table 1.

Table 1 Processing strategies at the service and user side for PPP/-AR/-RTK

Modeling	Strategies
Observation combination	Raw double-frequency
Orbits/Clocks/Phase bias	GFZ final orbit/clock products, estimated biases CNES real-time orbit/clock/biases products
Ionosphere corrections	Iono-float: estimated as unknown parameter Iono-weight: Interpolated from network side
Zenith troposphere delay	Estimated as random walk parameter
Satellite DCB	Corrected using products provided by DLR
Receiver DCB	Estimated as constant unknown parameter
Elevation cutoff	7°
Sampling	30 s
Coordinates	Service side: Static User side: Kinematic

Initial analysis of PPP and PPP-AR convergence

Fig. 1 shows 56 EUREF permanent stations selected for the convergence analysis. All stations were processed in the ambiguity-float and ambiguity–fixed solution without external ionospheric corrections or constraints. The coordinates from the EUREF weekly solution are selected as the reference, the positioning errors for all stations at each epoch are computed and sorted. Then the 50% percentage positioning errors are selected to indicate the convergence time.

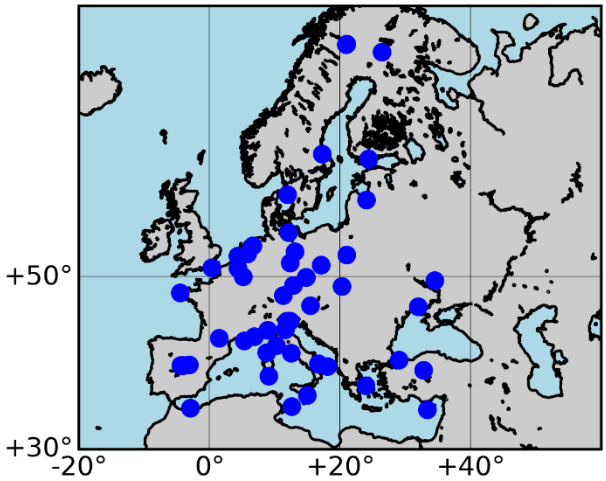

Fig. 1 Stations used for assessing PPP convergence and ionospheric accuracy

It can observed from Fig. 2 and Fig. 3 that the convergence time differs significantly when data from different stations are used along with different precise products. Overall, the solutions from the simulated real-time products show better performance than the CNES real-time products. This can be attributed to more precise final products together with phase biases estimated in the simulated real-time mode. The average PPP convergence time for the CNES and GOP ambiguity-float solutions for achieving the accuracy of a decimetre is 30min and 20min, respectively. It has been improved by 20% and 35% for the ambiguity-fixed solution, i.e. reaching 24min and 13min, respectively. Besides the accuracy, solutions' reliability have been improved by ambiguity fixing.

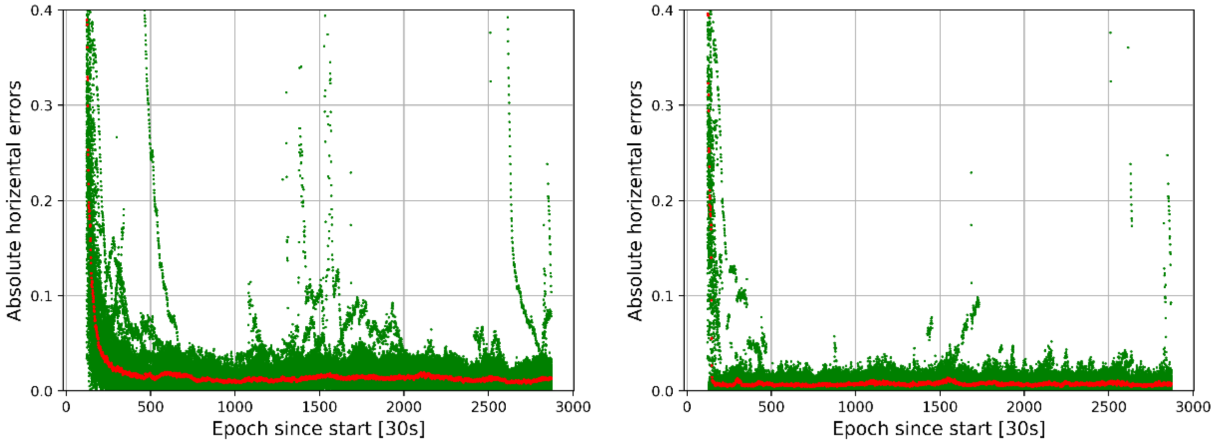

Fig. 2 Horizontal positioning errors achieved using PPP ambiguity-float (left) and ambiguity-fixed (right) using GFZ/GOP products: all errors (green), and 50% errors (red)

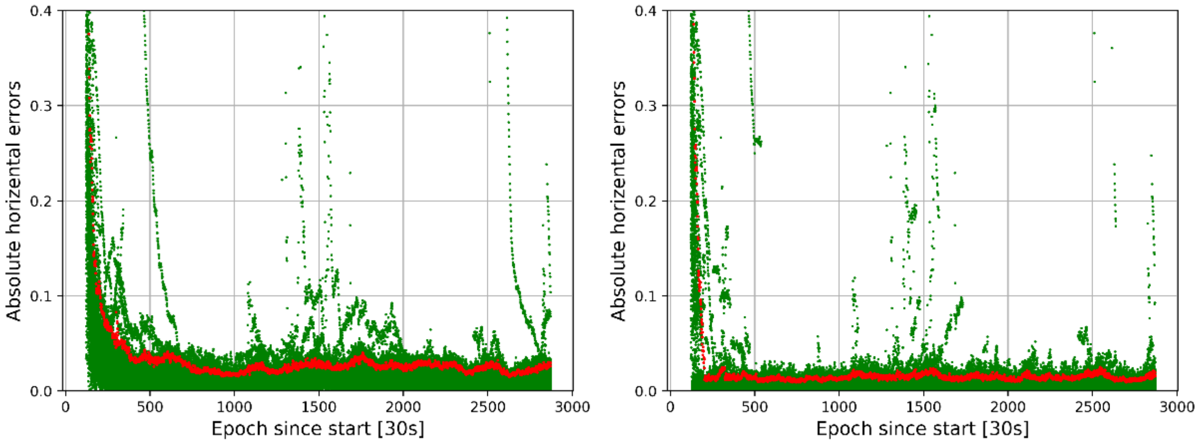

Fig. 3 Horizontal positioning errors achieved using PPP ambiguity-float (left) and ambiguity-fixed (right) using CNES products: all errors (green), and 50% errors (red)

Accuracy assessment of ionospheric delays

For assessing the performance of estimated ionospheric delays from the PPP-AR solution, short baselines were formed from three collocated stations: GOP6, GOP7 and GOPE. In theory, the single difference of the short baseline ionospheric delay should be close to zero, therefore a fluctuation of the single differenced ionospheric delay around zero can be used to measure systematic errors and random noise of the estimated ionospheric delays.

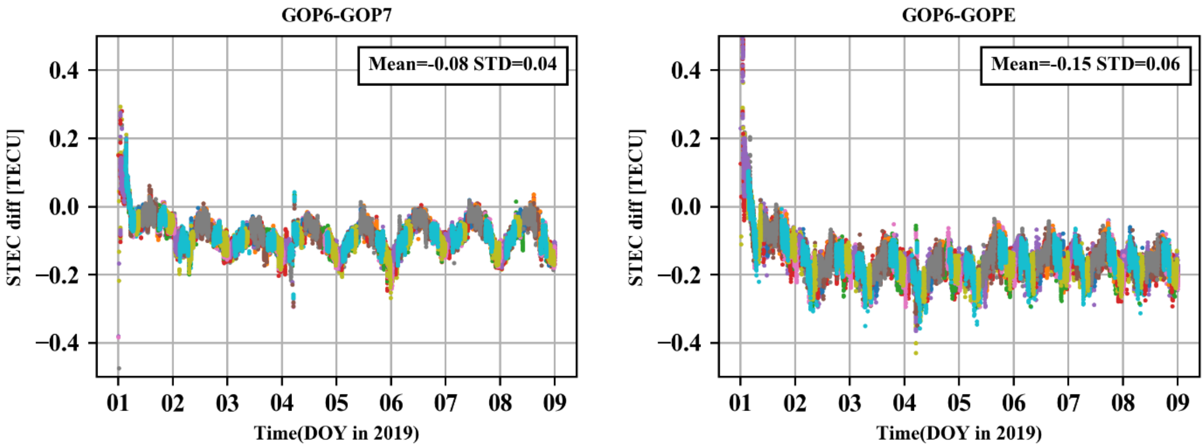

Fig. 4 Accuracy of the ionospheric delay derived from ambiguity-fixed solution

Fig. 4 shows the errors of ionospheric delays obtained from DOY (Day of Year) 001 to 008, 2019 using two short baselines GOP6-GOP7 and GOP6-GOPE. Note that only the ionospheric delays derived from the ambiguity-fixed solution are shown in the figure. It can be observed that the mean bias and the standard deviation (STD) of ionospheric delays derived from the ambiguity-fixed solution is within 0.15 TECU and 0.06 TECU, respectively. The results indicate a high quality of the estimated ionospheric delays, although a daily periodic term is still visible which correlates with the ionospheric activity.

The ionospheric delays estimated from the simulated real-time ambiguity-fixed PPP are selected as a reference, the accuracies of the interpolated ionospheric delay from the CODE global IONEX products (Dach et al, 2016) are evaluated on a station-satellite basis for all the ambiguity-fixed epochs of the daily observations. The calculated ionospheric error are shown in Fig. 5. It can be observed that the satellite G04 and G18 shows relatively large ionospheric errors. Besides, stations WARN and LEIJ also show a worse ionospheric accuracy which is caused mainly by the fixing rate of the ambiguity resolution.

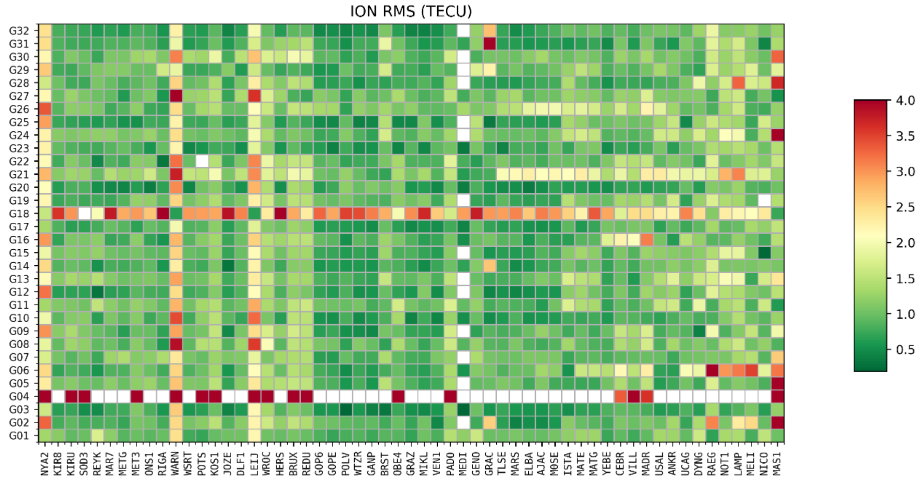

Fig. 5 Accuracy of the interpolated ionospheric delay from IONEX products with the ionospheric delays computed from PPP-AR as reference

The PPP convergence is expected to be shorten when using external ionospheric products. Hence, the final global vertical ionospheric product from CODE was introduced with a priori constraints for estimating PPP re-convergence on an hourly basis, i.e. with a regular resetting of all the estimated parameters. The convergence of the 50% positioning errors is analysed in Fig. 6. Different initial variances were used for constraining ionospheric parameters. The S00 option represents the PPP without using external ionospheric products, the S01, S03 and S05 options represent then initial ionospheric variances of 0.1, 0.3 and 0.5 m, respectively. It can be clearly observed that the positioning accuracy of the convergence period can be improved using external ionospheric delays. However, it is also clear that a higher weight for external ionospheric corrections (S01) may degrade the positioning. A similar convergence time is observed for the S03 and S05 solutions, while the S05 solution shows slightly better initialization of the position within each session.

A significant difference can be observed for the convergence time comparing different hourly solution. The PPP results between 09:00 and 15:00 (GPS time) show a longer convergence time. Fig. 7 presents the ionosphere variations from the station GOP6 which characterises an ionospheric activity within the processing session. Sessions with longer convergence time (Fig. 6) correspond to higher ionospheric activities (Fig.7). The 50% solutions from all the processed stations achieved a horizontal accuracy better than a decimetre within 5 min and 15 min within a low and high ionospheric activity, respectively.

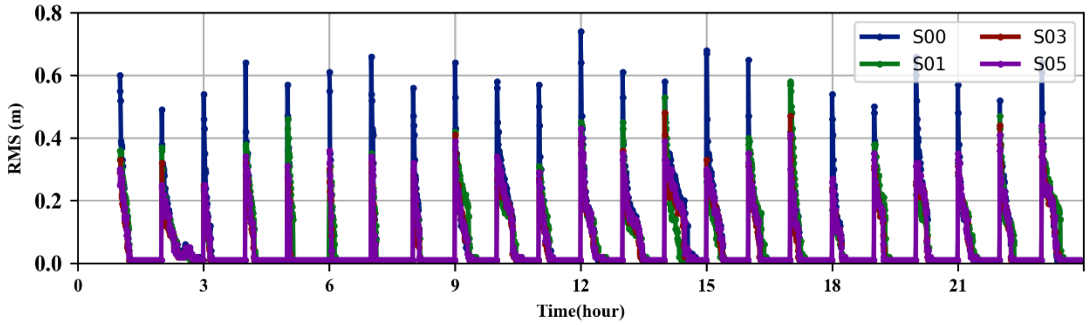

Fig. 6 Horizontal positioning errors of hourly PPP solutions using different a priori constraints for external ionospheric corrections

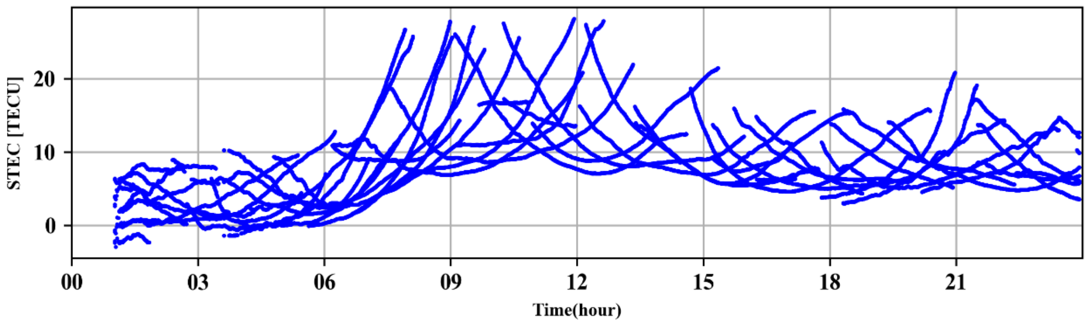

Fig. 7 Ionosphere variability from ambiguity-fixed PPP at station GOP6

PPP-RTK supported with ionospheric corrections

Fig. 8 shows stations selected for demonstrating PPP with a fast ambiguity resolution (PPP-RTK). For a user location (GOP6 station), ionospheric delays are interpolated from four reference stations with inter-station distances larger than 73km. Although the distance between GOP6 and LINZ is as long as 182km, the ionosphere modelling can still profit from a better spatial geometry of available ionospheric pierce points. Fig. 9 shows inter-station ionospheric errors derived by comparing the ambiguity-fixed ionospheric delays between the reference and the user stations. The STD of ionospheric errors achieved 0.18-0.45 TECU for inter-station distances of 73-182km. Mean biases of the ionospheric errors are not related to the inter-station distance, but these are attributed to hardware-related biases. The interpolated ionospheric errors for the station GOP6 were compared to the ambiguity-fixed ionospheric delays (estimated), see Fig. 10, and the mean bias and STD resulted in -0.01 TECU and 0.12 TECU, respectively. Compared to the accuracy of ionospheric delays between reference stations, the interpolation can still improve the accuracy of the ionospheric delay which will be beneficial for the PPP-RTK.

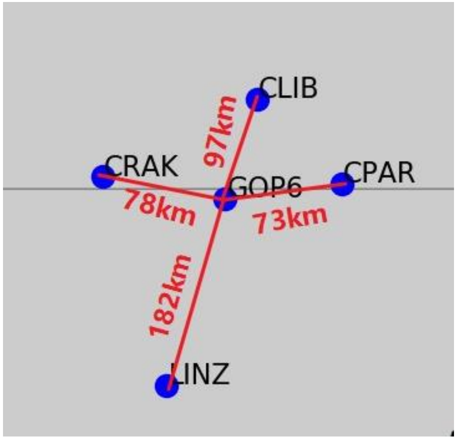

Fig. 8 Station distribution and inter-station distance used in PPP-RTK demonstration

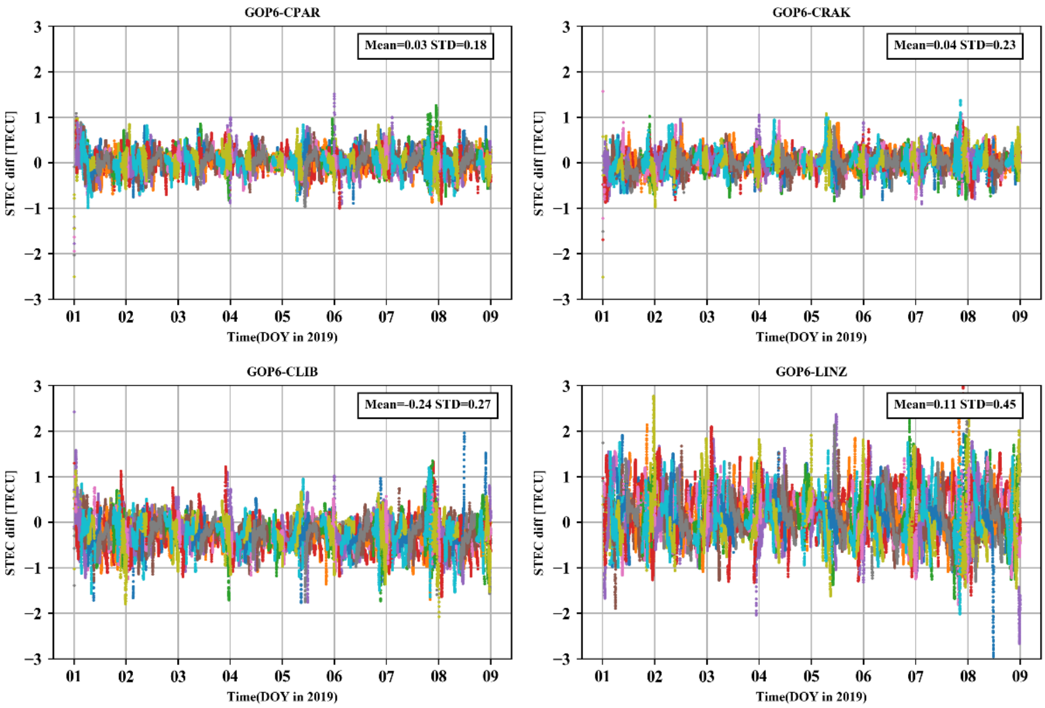

Fig. 9 Inter-station ionospheric errors between reference stations and a user station

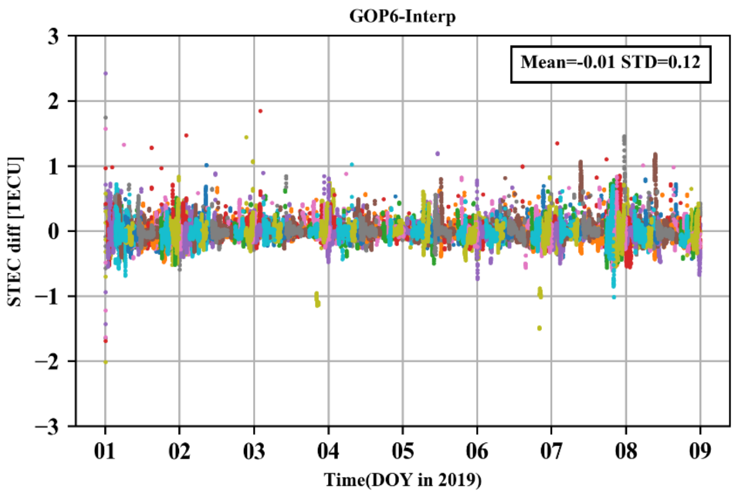

Fig. 10 Interpolated ionospheric errors at a user station

Hourly PPP observations from DOY 001, 2019 were used to evaluate the performance of the PPP-RTK at the station GOP6, i.e. with a fast ambiguity resolution. An empirical variance of 0.15m was used for a priori constraining of external ionospheric corrections. Fig. 11 shows a comparison of the PPP-AR without applying ionospheric correction, and with applying ionospheric correction from the nearby station GOPE. In most hourly sessions, the ambiguity resolution in the PPP-RTK was achieved within two epochs when a sampling interval of 30s was applied. Besides the positioning accuracy, the correct ambiguity fixing is largely improved. Fig. 12 then compares the solution using the ionospheric corrections estimated from the station GOPE and using the interpolated corrections. A similar performance can be observed when using the two different corrections, but slightly better initial positions when using corrections estimated nearby (from GOPE). The results illustrate a high precision of the ionospheric delays interpolated from selected reference stations and a feasible approach for such empirical stochastic ionosphere modelling.

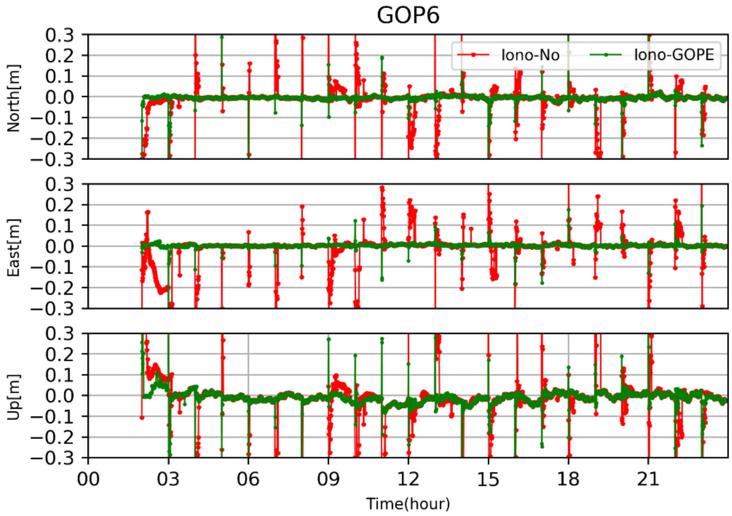

Fig. 11 Position errors of ambiguity-fixed PPP without external ionospheric delay and with ionospheric corrections estimated at nearby station GOPE

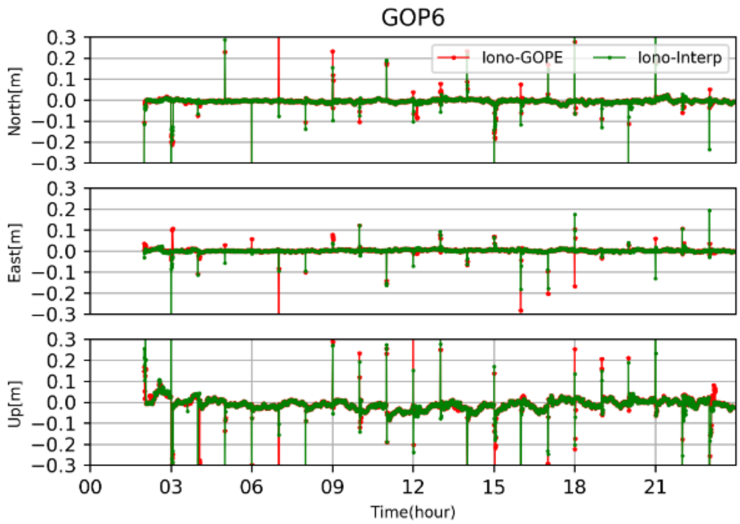

Fig. 12 Positioning errors for ambiguity-fixed PPP using ionospheric corrections from nearby station GOPE and corrections interpolated from selected reference stations

Besides, a reference network with longer inter-station distances (209 – 413km) were selected to demonstrate the impact of larger networks on the PPP-RTK. The station GOP6 was also selected as the reference on DOY 001, 2019. The distribution of the stations and the accuracy of the interpolated ionospheric errors are shown in Fig. 13. Results indicates that the STD of the ionospheric delay is 0.22 TECU. It is worse than the previous results, see Fig. 10, and it is attributed to the longer inter-station distances. After applying new interpolated ionospheric corrections to the PPP-RTK, Fig. 14 shows results comparing the ambiguity-fixed solution with and without external ionospheric corrections. A slightly worse performance was obtained during the first two hours of the solution which is attributed mainly to the convergence precision of the ionospheric delays. A fast ambiguity resolution can be achieved within several epochs using such external ionospheric corrections. Both the correct ambiguity fixing rate and the positioning accuracy has been improved.

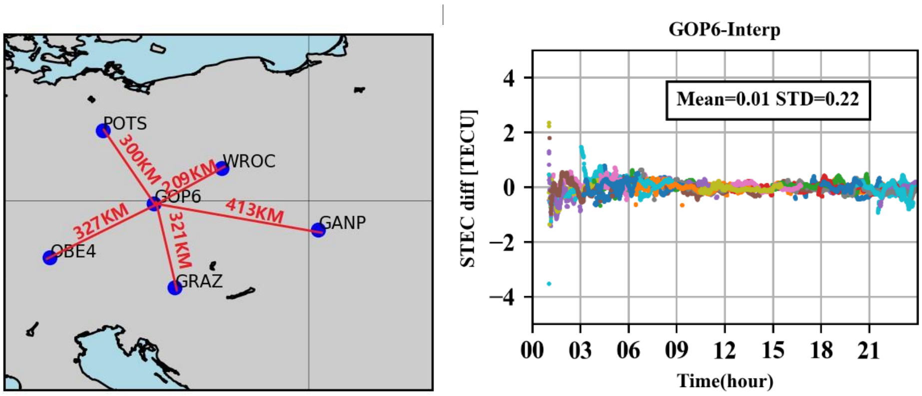

Fig. 13 Comparison of interpolated ionospheric delay for station GOP6

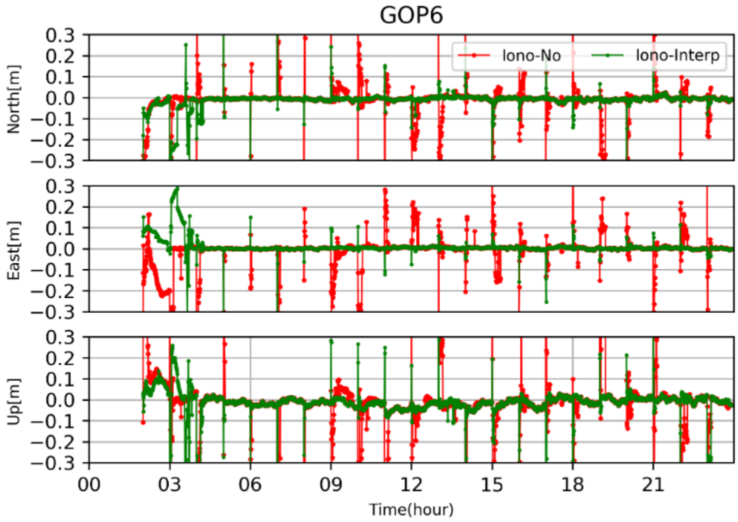

Fig. 14 Position errors for ambiguity-fixed PPP using ionospheric corrections interpolated from stations in distances above 209km

Fig. 15 shows the performance of Galileo-only PPP ambiguity resolution without external ionospheric corrections (Iono-No) and with interpolated ionospheric corrections (Iono-Interp). The ambiguity fixing rate is improved although results were worse than that of GPS which might be still attributed to lower number of Galileo satellites and thus worse solution geometry.

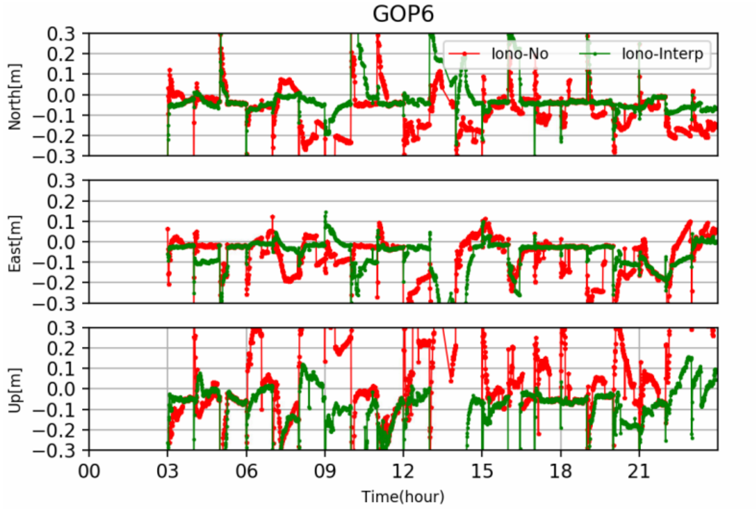

Fig. 15 Position errors for ambiguity-fixed PPP using Galileo observations

CONCLUSIONS

PPP-RTK shares the benefit of PPP that can achieve a high precision accuracy on a global scale with a single receiver and the benefit of RTK that can achieve a fast convergence. The performance of the GPS and Galileo-only PPP-RTK are evaluated based on data of the EUREF regional network. For traditional ambiguity-float PPP, an averaged convergence time of 30 min and 20 min is needed for the horizontal and vertical positioning accuracy to convergence to decimetre level with the 50% probability. After applying the ambiguity-fixing methods, the convergence time reduced to 24min and 13min, respectively.

Precise ionospheric corrections are the key prerequisite for achieving fast ambiguity resolution in PPP-RTK. The mean bias and standard deviation of the ionospheric errors derived from the ambiguity-fixed PPP are within 0.15 TECU and 0.06 TECU based on the short-baseline test. But a daily periodic term exists in the ionospheric error series. The PPP-RTK experiments based on the GPS observations with the inter-station distance range from 73 km to 209 km indicated that the ambiguity fixing can be achieved within several epochs. The performance of Galileo-only PPP-RTK is worse than that of GPS, but the accuracy and the ambiguity fixing rate can be largely improved with external ionospheric correction.

REFERENCES

Bruyninx, C., Legrand, J., Fabian, A., Pottiaux E. (2019) GNSS metadata and data validation in the EUREF Permanent Network, GPS Solut. 23:106, doi:10.1007/s10291-019-0880-9

Dach R, Schaer S, Arnold D, et al. CODE final product series for the IGS[J]. 2016.

De Oliveira P S, Morel L, Fund F, et al. Modeling tropospheric wet delays with dense and sparse network configurations for PPP-RTK[J]. GPS solutions, 2017, 21(1): 237-250.

Deng, Z., Fritsche, M., Uhlemann, M., et al., Reprocessing of GFZ multi-GNSS product GBM. In: IGS Workshop 2016, Sydney

G. Wubbena, M. Schmitz, and A. Bagge, “PPP-RTK: Precise Point Positioning using state-space representation in RTK networks," in Proceedings of ION GNSS, 2005, vol. 5, pp. 13–16.

Ge, M., Gendt, G., Rothacher, M., et al.: Resolution of GPS carrier-phase ambiguities in precise point positioning (PPP) with daily observations. J. Geodesy 82(7), 389–399 (2008)

Geng, J., Teferle, F.N., Meng, X., et al.: Kinematic precise point positioning at remote marine platforms. GPS Solutions 14(4), 343–350 (2010)

Laurichesse, D.; Blot, A. Fast PPP convergence using multi-constellation and triple-frequency ambiguity resolution. In Proceedings of the ION GNSS 2016, Portland, OR, USA, 12–16 September 2016.

Li Z, Chen W, Ruan R, et al. Evaluation of PPP-RTK based on BDS-3/BDS-2/GPS observations: a case study in Europe[J]. GPS Solutions, 2020, 24(2): 1-12.

Li, X.; Zhang, X.; Ge, M. Regional reference network augmented precise point positioning for instantaneous ambiguity resolution. J. Geod. 2011, 85, 151–158.

Psychas D, Verhagen S, Liu X, et al. Assessment of ionospheric corrections for PPP-RTK using regional ionosphere modelling[J]. Measurement Science and Technology, 2018, 30(1): 014001.

Psychas D, Verhagen S. Real-time PPP-RTK performance analysis using ionospheric corrections from multi-scale network configurations [J]. Sensors, 2020, 20(11): 3012.

Teunissen, P.J.G.; Odijk, D.; Zhang, B. PPP-RTK: Results of CORS network-based PPP with integer ambiguity resolution. J. Aeronaut. Astronaut. Aviat. 2010, 42, 223–230.

Václavovic, P., Douša, J., Gyori, G. (2013) G-Nut software library - state of development and first results, Acta Geodyn. Geomat. 10:4(172), 431-436, doi:10.13168/AGG.2013.0042

Zhang, B.; Teunissen, P.J.G.; Odijk, D. A Novel Un-differenced PPP-RTK Concept. J. Navig. 2011, 64,S180–S191.

Zumberge. J.F., Heflin, M.B., Jefferson, D.C., Watkins, M.M., Webb, F.H. (1997) Precise point positioning for the efficient and robust analysis of GPS data from large networks J. Geoph. Res. (Solid Earth), 102:5005-5017